A strategy for material characterisation of multi-wythe masonry Infrastructure Preliminary study

Li, Xi; Esposito, Rita

DOI
10.1016/j.conbuildmat.2023.133600

Publication date
2023

Document Version
Final published version

Published in
Construction and Building Materials

Construction and Building Materials 408 (2023) 133600

Contents lists available at ScienceDirect

Construction and Building Materials

journal homepage: www.elsevier.com/locate/conbuildmat

A strategy for material characterisation of multi-wythe masonry Infrastructure: Preliminary study

Xi Li *, Rita Esposito

Faculty of Civil Engineering and Geosciences, Delft University of Technology, Stevinweg 1, 2628CN, Delft, the Netherlands

ARTICLE INFO

Keywords:
Multi-wythe masonry
Core testing method
Through-thickness effect
Nonlinear behaviour
Dutch urban infrastructure

ABSTRACT

The present work aims at providing insights on the material characterization of multi-wythe masonry infrastructure, in particular exploring a through-thickness effect of mechanical properties and benchmarking the core testing as an efficient slightly-destructive testing method. An experimental campaign was carried out to characterize shear, compressive and bond properties of a 1.2-m thick bridge's pillar constructed in 1882 in the city of Amsterdam (the Netherlands). Both cores and rectangular samples (e.g. prisms, triplets, couplets) were extracted across different locations in the wall thickness to evaluate the effect of exposure to environment conditions and to verify the capability of core testing methods. Results show that the masonry close to the water side (external) showed higher values of elastic modulus and lower values of flexural bond properties with respect to masonry inside the pillar. As for the capability of core testing on multi-wythe masonry, generally cores would present similar compressive/shear properties compared with rectangular samples. Besides, bond patterns and dimensions of cores showed negligible effect on compressive properties; However, this needs to be extensively verified by considering other masonry typologies. Overall, the study provides a first insight on the mechanical properties of multi-wythe masonry urban infrastructure and knowledge regarding the sampling and testing strategy for these structures. In turn, this will increase the knowledge on multi-wythe masonry, which is limited in literature, and will support the assessment of many infrastructure in typical Dutch canal cities by providing input for calculation methods.

1. Introduction

Over 200 km of quay walls and several bridges are in urgent need of renovation in the city of Amsterdam [1]. Nowadays, these brick masonry structures do not only represent an important infrastructure for the viability of the city, but they are also important historical assets. In recent years, bridges and quay walls showed substantial deformation and in some cases even collapse, e.g. [2,3]. Pillars and abutments of bridges as well as quay walls generally have a large thickness (from 600 to more than 1000 mm) and especially the oldest constructions are made of multi-wythe brick masonry fully bonded through the thickness. Very limited knowledge is available on the material characterisation of these unreinforced masonry structures, thus reducing the reliability of their structural assessment. To accurately evaluate the remaining service life of these structures, nonlinear finite element analyses able to account for redistribution of forces within the masonry superstructure are required [4]. These models require the complete characterisation of nonlinear behaviour of masonry and its constituents (i.e. brick and mortar). Additionally, considering the different exposure conditions of the masonry, i.e. above and below water, or external (water-side/soil-side) and internal, possible differences in mechanical properties may be expected. Therefore, it is necessary to perform experimental tests on these old masonry structures, to characterise their mechanical properties and to provide the definition of input parameters for nonlinear finite element analyses.

The major challenge in the characterisation of mechanical properties of masonry for existing (infra)structures is finding the balance between invasiveness of the sampling/testing area and the level of knowledge acquired (e.g. complete or partial definition of nonlinear behaviour). Recently, among others operational modal analysis as an advanced technique can assess health conditions of in-service masonry infrastructures in the real time regarding elastic properties, local damage or diffused surface decay [5–7]. However, for a comprehensive characterization of material properties, core testing on small-diameter cylindrical samples has shown a great potential for existing single-wythe masonry buildings, e.g. [8–12]. It provides possibilities of acquiring

* Corresponding author.
E-mail addresses: xi.li@tudelft.nl (X. Li), r.esposito@tudelft.nl (R. Esposito).

https://doi.org/10.1016/j.conbuildmat.2023.133600
Received 14 June 2023; Received in revised form 19 September 2023; Accepted 29 September 2023
Available online 5 October 2023

both the pre- and post- peak behaviour of masonry under shear and compressive loadings. To characterise shear properties at brick–mortar interfaces, I-shaped cores with one bed joint are usually rotated at different inclination angles for performing splitting tests [9,12–14]. The effect of inclination angles (0° - 50°) on the failure modes of cores was investigated by Mazzotti et al. [12]. They recommended using cores with a high mortar joint inclination (40°-50°) for splitting tests as the most representative failure mode for masonry, i.e. sliding failure mode, can be exhibited rather than splitting tensile mode across both brick and interface. Jafari et al. [9] performed splitting tests on I-shaped cores for various masonry types and compared the results about shear properties with the ones from shear-compression tests on triplets. They found a correlation coefficient between results of core and triplet tests of 0.88 for initial shear strength and 0.96 for friction coefficient. To characterise the compressive properties of masonry, example of cylindrical samples with different diameters, thickness and bond patterns can be found in literature [8,10,15]. To achieve a uniform stress distribution under compression, specimens are capped at top and bottom. Early research employed steel cap [16,17], but recent research showed that a high-strength mortar cap is more appropriate to avoid over-constraining the masonry specimen [18]. A debate is still open regarding the shape and size to be selected and the correlation coefficient to be used to relate results to the one of standard compressive tests on wallets and prisms. Segura et al. [15] concluded that the compressive strength and the Young's modulus were, respectively, 25 % and 15 % higher for I-shaped cores with a diameter of 90 mm with respect to H-shaped cores (two bed joints and one head joint) with a diameter of 150 mm. Dorji et al. [19] extracted cores of 150 mm diameter with four different types of bond patterns from old masonry arch bridges, and they found that the increased number of head joints in masonry cores decreased the masonry compressive strength. However, Jafari et al. [10] did not find substantial difference in Young's modulus and compressive strength obtained between T-shaped cores (one bed joints and one head joint) with a diameter of 100 mm and H-shaped cores with a diameter of 150 mm, and they obtained a 1:1 correlation with the results of tests on wallet. On the contrary, different results in terms of compressive fracture energy and strain at peak were obtained between the various types of cores and wallets. In comparison with standard tests on wallet, Sassoni et al. [20] observed 20–35 % higher compression strength for cores, and they concluded that this overestimation of strength is attributed to the confining action exerted by mortar castings beneath and above the cores. Despite the various differences reported in literature, the core testing method seems to be the most efficient approach for the material characterisation of existing (infra)structures considering the potentiality to obtain both pre- and post- peak properties under shear and compressive loading, with limited sampling volume and easy extraction method. Additionally, this gives the advantage that in case of composite structures, i.e. masonry/reinforced concrete walls or presence of renovation, the same samples can be adopted independently of the construction material. Nevertheless, more research is needed to evaluate its applicability to multi-wythe masonry for urban infrastructures, since most of study cases refers to single-wythe/double-wythe masonry in buildings [21–23].

At present, limited research is available on material characterisation of multi-wythe masonry. Demir and Ilki [24] compared the damage evolution and mechanical properties of multi-wythe and single-wythe masonry prisms under compression. They found that multi-wythe prisms present vertical cracks along the interfaces of the external and internal wythe for lower imposed deformation; besides, the overall axial deformability is significantly higher and the compressive strength is almost halved. Until now, we are still lack of a comprehensive understanding about material characterisation of multi-wythe masonry walls under various loading conditions like shear, compression, and bending. As a result, an experimental strategy for the evaluation of such thick structure is urgently needed. Regarding the through-thickness effect of multi-wythe masonry, the potential variation of mechanical properties in the wall thickness has been rarely studied. Franzoni et al. [25] tested masonry triplets in dry moist and water-saturated conditions; they observed that the moist condition has the worse effect on compressive strength than the water-saturated and the dry condition. Sathiparan and Rumeshkumar [26] noticed a significant reduction of shear and bond strength (10 %-20 %) for masonry prisms in wet condition. Therefore, it is necessary to experimentally evaluate the possible variation of mechanical properties through the thickness direction due to the exposure to different environmental conditions, for better serving the non-linear structural analysis on the multi-wythe masonry [4,27].

To provide insights on how to characterise multi-wythe brick masonry infrastructure, a pilot study has been started at Delft University of Technology in 2022 with the characterisation of a bridge's pillar built in 1882 in Amsterdam (the Netherlands). Samples were extracted in the portion of masonry above water level and different samples through the thickness direction of the masonry wall were collected. Various mechanical tests, including tests on cores and on rectangular samples (e.g. couplets, prisms, triplets) were performed. In this paper, the outcome of compressive tests on cores and prisms, splitting tests on cores, shear-compression tests on triplets, and bond wrench tests on couplets, are presented to characterise compressive properties of masonry as well as shear and bond properties of brick–mortar interfaces. The primary scope of this paper is to identify if it exists a variation of the mechanical properties throughout the thickness and to discuss the suitability of the core testing method for multi-wythe brick masonry in urban infrastructure.

2. Materials and methods

2.1. Materials and sample extraction process

During the renovation of a bridge in the city of Amsterdam, a portion of masonry with dimensions 0.6 × 1.4 × 1.2 m^3 (length × height × thickness) was extracted from a pillar originally built in 1882, as shown in Fig. 1(a)-(c). The extraction took place in April 2020; afterwards the portion was caged in a steel box and stored in uncontrolled conditions. The portion of masonry is made of solid clay bricks having on average a length of 210 mm, a width of 100 mm and a height of 50 mm, and of mortar joints having a thickness ranging from 2 mm to 20 mm. The solid clay brick is made of clay from the Old Rijn or Utrecht, while the type of mortar is a cement-lime mortar which is made of shell lime, latent hydraulic binder (cement and trass), sand in the proportion (by volume) of 5:3:1or 5:2:2 according to archive research [28,29]. Regarding the bond pattern, the front side of the masonry wall is built in Dutch bond (a row of headers alternated to a row of stretchers), Fig. 1(b); however, through the thickness direction the internal bricks were mainly laid as headers although a clear bond pattern was not identified. Table 1 lists the properties of brick and mortar obtained accordingly to NEN-EN 772–1 [30] and DIN 18555–9 [31], respectively. Here, the compressive strength of bricks is obtained based on a shape coefficient of 0.75 according to NEN-EN 772–1 [30], considering the dimension of tested samples was approximately 210 mm × 100 mm × 50 mm (after capping was applied). After sawing the portion of pillar in piece, it was noticed that a limited amount of bricks in their full size was available since mostly header bond pattern was used throughout the thickness. This reduced the maximum number of tests per piece to 3. For the double-punch test on mortar, the specimens had an irregular form which was larger than the recommended dimensions (40 × 40 mm); generally, a minimum diameter of 45 mm was observed. The compressive strength of mortar joints was estimated as the maximum force divided by the area of the punch with a diameter of 20 mm. The surface of both bricks and mortar joints was capped with a thin layer of gypsum for a better contact with the loading plates or punches under compression.

The extraction of samples for material characterisation took place in 2022 and the procedure consisted two phases. In the first phase, the masonry portion was sawed along the thickness using diamond blades

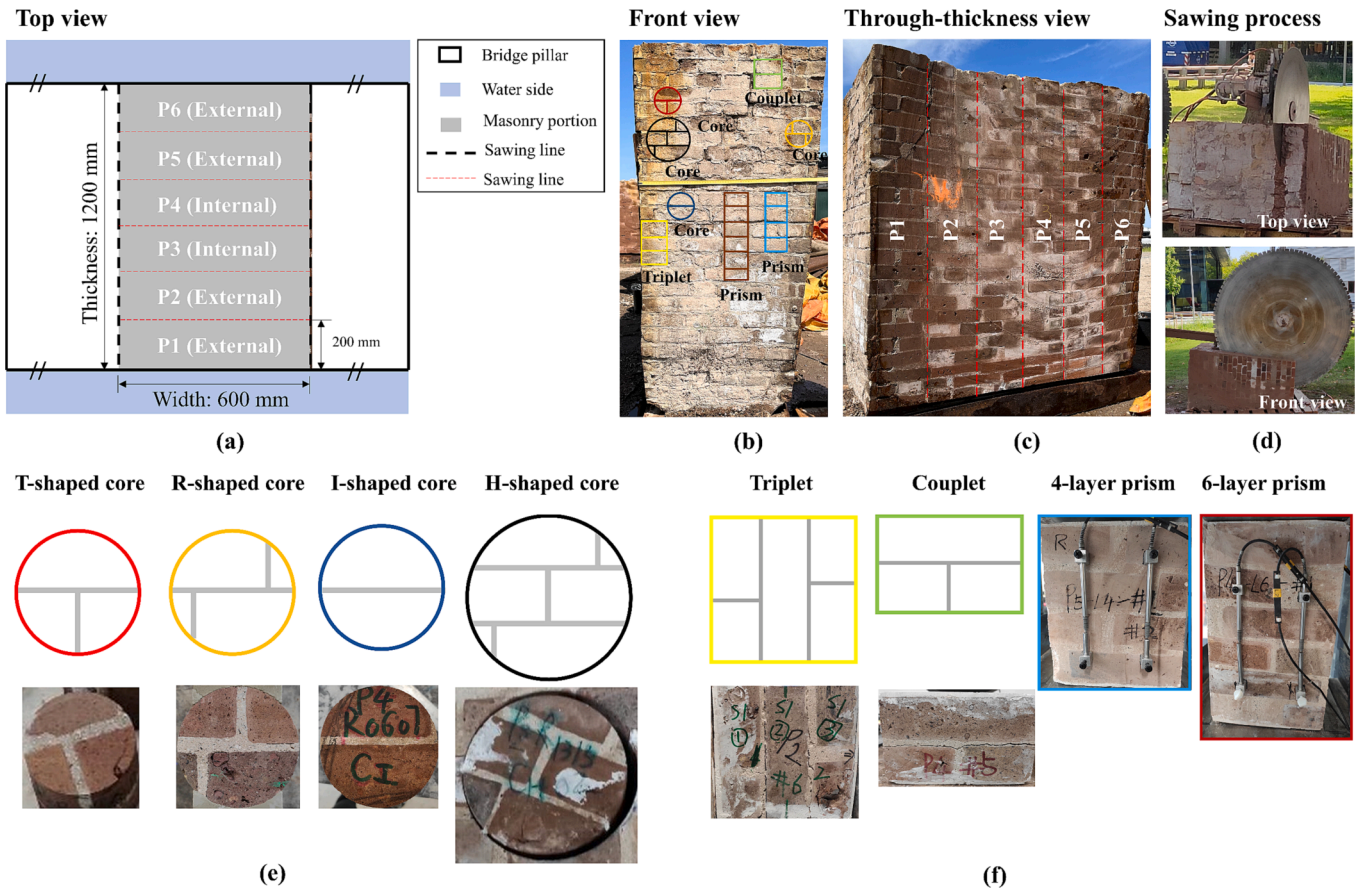

Fig. 1. Top view of the masonry portion (a); Front view of the masonry portion (b); Through-thickness view of the masonry portion (c); Sawing process to obtain P1-P5 (d); Different types of cores extracted from P1-P5 (e); Different types of standard rectangular samples extracted from P1-P5 (f).

Table 1
Compressive properties of bricks and mortar.

Masonry unit	Wall portion	Number of samples	Compressive strength (MPa)	C.o.V. (%)
Brick	P2	3	26.71	28
Brick	P4	3	26.78	16
Mortar	–	7	7.61	13

Table 3
An overview of the number of rectangular samples from P2, P4 and P5.

Type of sample Wall portion	Triplets	Couplets	Prisms (6-layer brick)	Prisms (4-layer brick)	Bricks
P2	6	4	–	–	3
P4	–	4	4	3	3
P5	–	–	4	4	–

Table 2
Summary of bond pattern, dimension and number for cores in different groups presented in Fig. 1.

Group ID	Wall portion	Bond Pattern	Diameter (mm)	Thickness (mm)	Number of samples
P1-T-S	P1	T	100	60–100	5
P1-R-S		R	100	60–100	3
P1-I-S*		I	100	60–100	1
P2-T-S	P2	T	100	60–100	4
P2-R-S*		R	100	60–100	2
P2-I-S		I	100	60–100	3
P3-T-S	P3	T	100	60–100	5
P3-R-S*		R	100	60–100	2
P3-H-D		H	150	~200	4
P3-R-D		T/R	100	~200	5
P3-I-S		I	100	60–100	4
P4-T-S*	P4	T	100	60–100	2
P4-I-S		I	100	60–100	8

Note: * denotes that only two samples were obtained during the extraction.

(Fig. 1(a), (c) and (d)), so that 6 pieces (P1-P6) should be obtained with average dimensions of 600 × 1200 × 200 mm^3. However, extraction of samples from P6 would not be possible due to the absence of support for the large blade. Consequently, smaller pieces were extracted from P6 by means of manual sawing to preserve the integrity of P5. Eventually, this limited testing for P6. In the second phase, a wet extraction procedure as in the first phase was employed to drill cores and cut rectangular samples as prisms, triplets and couplets (Fig. 1 (e) and (f)). The random bond pattern of the masonry bridge along the thickness direction makes it hard to drill cores and extract rectangular with a specific pattern of mortar joints. Thus, the number of samples is limited for some tests in the present study. In Table 2, the extracted cores from P1-P4 are classified in 13 groups named as "wall portion-bond pattern-single/double wythe", where the bond patterns are showed in Fig. 1 (e). The following letters are used: "T" indicates cores with one bed joint and one head joint; "R" identifies cores with one bed joint and two head joints; "I" indicates cores with one bed joints; "H" identifies cores with two bed joint and three head joints. Besides, single-wythe cores here refers to the ones without collar joints, while double-wythe cores refers to the ones with one collar joint. The varying range of thickness of single-wythe cores is caused by the removal of collar joints after the drilling process. In Table 3, the number of rectangular samples extracted from P2, P4 and P5 is listed for each type. This list includes triplets and couplets constitute of vertically stacked three-layer or two-layer bricks, respectively. Triplets always presented a full brick in the centre, while couplets had a full brick at the top side (Fig. 1 (f)).

In view of the limited variation of brick strength between the various pieces (Table 1) and the results of a visual inspection, it is assumed that the masonry of the pillar's portion considered is of the same typology. Here, a masonry typology is a masonry made of the same bricks and mortar type, built with the same bond pattern in a specific time. Considering a possible variation of the properties based on the exposure conditions (e.g. close to or far of the water), it was assumed that two masonry objects could exist: an external one (P1, P2, P5 and P6), and internal one (P3 and P4). Here, a masonry object is identified as masonry of the same typology subjected to the same exposure condition. This classification was made a posteriori by considering the observed variation of the mechanical properties. Additionally, extraction and transportation of the masonry portion in the steel cage may have cause damage to P1 and P6, which were indeed characterised by several

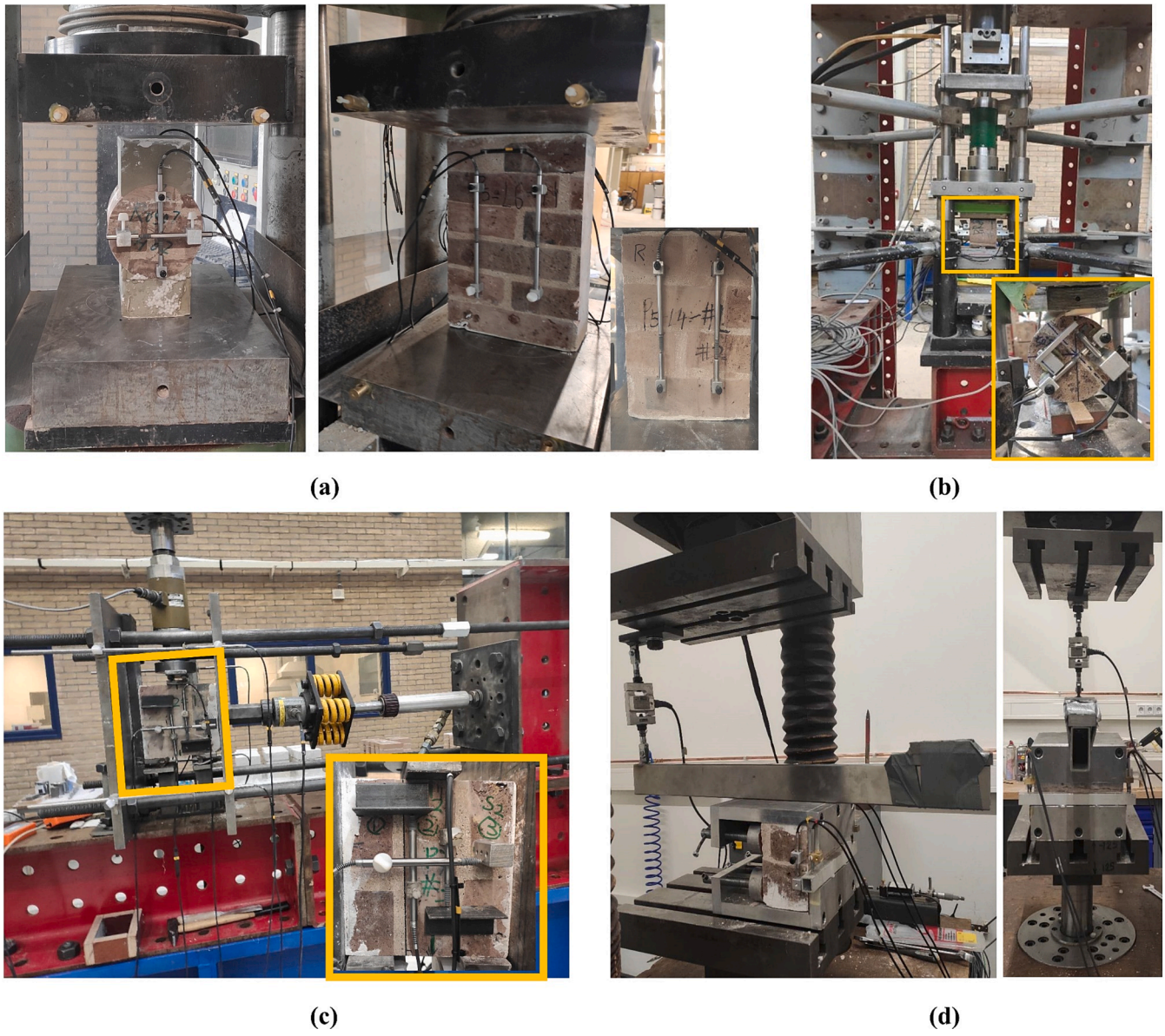

Fig. 2. Test set-ups: (a) compressive tests on cores and prisms; (b) splitting tests on cores; (c) shear-compression tests on triplets; (d) bond wrench tests on couplets.

surface cracks.

2.2. Testing procedures for determining compressive properties

To evaluate the compressive properties of masonry, two main types of tests were used: tests on cores accordingly to Jafari et al. [10] and tests on prisms following ASTM C1314-09 [32]. This choice was made to evaluate the applicability of core testing method to multi-wythe masonry infrastructure considering that the method resulted in efficient and reliable estimation of the complete nonlinear behaviour of single-wythe masonry [9,10] with limited invasiveness of sampling. Tests on prisms were adopted as benchmark for core testing. Correlation factors of compressive properties from prims and wallets, e.g. 0.75 for strength suggested by Thamboo and Dhanasekar [33], can be further applied to check the differences of test results from cores and wallets. Considering the thickness of the wall, both single-wythe (without collar joint) and double-wythe (with collar joint) masonry cores with different bond patterns were showed, as listed in Table 2. Due to the difficulties in predicting the bond pattern along the thickness of the wall, the single-wythe cores had a thickness ranging between 60 mm and 100 mm.

For both tests, a displacement-controlled testing machine with a 3500 kN hydraulic jack (Fig. 2(a)) was used to evaluate elastic, strength and fracture energy properties in compression. A monotonic test with a displacement rate of 0.002 mm/s was applied. Linear variable differential transformer (LVDT) with a measurement range of 10 mm was used to record the vertical deformation, except for cores with a diameter of 100 mm for which LVDTs with a measurement range of 2 mm were adopted. Additionally LVDTs with a measuring range of 10 mm were used to measure the horizontal deformation for cores, but the related measurements were not involved in the analysis considering the majority of LVDTs in horizontal position were detached from samples along with the horizontal expansion under compression. Three to five repetitive tests were carried out for most types of specimens from different masonry pieces, while few cases for cores only contain two repetitive tests due to the difficulties of sample extraction.

To apply a compressive load to the core, a high-strength mortar capping was used at the top and the bottom of the specimen (Cement Cuglaton Gietmortel 1 mm, mixing of 0.75 kg water per 5 kg). For different core diameters, the ratio between the cap width and the core diameter was kept constant to 0.7, while the ratio between the minimum height of the cap (at the centre) and the cap width is approximately 0.34. Consequently, the width and height of the cap are 70 mm and 50 mm for cores with a diameter of 100 mm, and 105 mm and 80 mm for cores with a diameter of 150 mm. Wooden moulds with a length of 100 or 200 mm were used for single- and double-wythe masonry cores, respectively. In case the core thickness is smaller than the mould length, clay or polystyrene material were used as fillings to the wooden mould. The capped cores were cured for 7 to 9 days at room temperature prior to testing. Under these conditions, the capping material shows a mean flexural strength of 5.5 MPa and a mean compressive strength of 61.37 MPa accordingly to EN 1015–11 [34]. For prisms and if needed also for cores, a layer of gypsum was used to flatten the contact surface between samples and loading plates.

For both tests, the complete stress–strain curve in axial direction and crack pattern evolution were analysed, as well as key mechanical properties were evaluated as proposed by Jafari et al. [22]. Due to detachment of LVDTs for large deformation, the axial strain was evaluated as follow: in the pre-peak phase the average of deformation from all vertical LVDTs (2 in the case of core testing and 4 in the case of prism testing) was considered, while in the post-peak phrase the deformation of the jack was considered correcting for its difference with LVDTs measurements [22]. The axial stress was calculated considering the cross-sectional area of the cap and of the prism for the core and prism testing, respectively. Once determined the stress–strain curve in the axial direction, the elastic modulus was calculated as the chord between 1/10 and 1/3 of the maximum stress according to ASTM E111(2017) [35] and previous work in our laboratory [22], to alleviate the effect of the gradual contact between the loading plates and the samples on the estimation of elastic modulus. The compressive strength was associated to the maximum stress and the corresponding strain was defined as the strain at peak. The compressive fracture energy was evaluated as the area under the stress versus strain curve; the curve was extended to zero stress considering a linear extrapolation of the strain [22].

2.3. Testing procedures for determining shear properties

To evaluate the shear properties at brick–mortar interfaces, two main test types were used: splitting tests on cores accordingly to Jafari et al. [9] and shear-compression tests on triplets accordingly to EN 1052–3 [36]. The tests were performed in displacement control to allow the evaluation of both initial and residual shear properties. Similarly as compressive tests, the aim is to evaluate the applicability of core testing method for multi-wythe masonry infrastructure using triplet tests as a benchmark.

Splitting tests were performed on I-shaped cores by inclining the mortar bed joint with respect to its original position (i.e. 45°, 50° and 55°). At least three samples were tested at each inclination for the splitting tests. The test was carried out by a sliding-controlled apparatus including a hydraulic jack with 100 kN capacity, as shown in Fig. 2(b). Two wooden strips, with dimension of 194 × 15 × 2 mm, were inserted between the loading plates and the sample to distribute the load. The relative sliding displacement and normal displacement between the two bricks were measured on each face of the specimen using LVDTs with a measuring range of + 2 mm. The average sliding measurements (between front and back face) was used to control the load. A sliding-displacement-rate of 0.0001 mm/s was adopted during the tests. The shear stress and the normal stress at the brick–mortar interface were evaluated from core testing as follows.

$$f_{v,core} = \frac{F}{A} sin\alpha \tag{1}$$

$$f_{p,core} = \frac{F}{A} \cos\alpha \tag{2}$$

where F is the force from the testing machine, A is the area of the mortar layer, and α is the mortar layer inclination, with respect to the horizontal reference (original position of bed joint). By considering the Coulomb friction criterion, the value of the initial shear strength $f_{v0,core}$ and the coefficient of friction μ_{core} were evaluated by a linear regression of the maximum shear and maximum compressive stresses obtained by tests on cores with different mortar layer inclinations. In literature, two methods are reported for the evaluation of the shear properties of masonry from core testing: the linear regression considering the average strength per each mortar inclination (as proposed by Mazzotti et al. [12] and adopted by Jafari et al. [9]), or the linear regression of all the data (as proposed by Pelà et al. [13]). In the present work, both methods are applied for comparison.

Shear-compression tests on triplets were performed at different pre-compression stresses, i.e. 0.2 MPa, 0.6 MPa and 1.0 MPa (EN 1052–3 [36]). Two samples per pre-compression level were tested. A displacement-controlled procedure was performed at a rate of 0.005 mm/s. Two actuators were used: a computer-controlled hydraulic jack with a capacity of 100 kN for the vertical load and a manually-operated hydraulic jack with a capacity of 50 kN for the horizontal load (Fig. 2 (c)). To minimise the variations of the horizontal force, springs with a stiffness of 3300 N/mm were used. The specimens generally showed a subsequent failure of the two joints leading to the presence of two peaks in the shear stress versus sliding displacement curve (Fig. 8). To evaluate the shear strength at each peak from the applied force, the area of only one brick–mortar interface was considered for the first peak, while the area of both interfaces was considered for the second peak. The shear stress versus sliding displacement curve showed a plateau for large

sliding displacement. The stress at the plateau was defined as the residual strength. If possible, the residual shear strength was evaluated at different level of pre-compression for the same specimen, similarly to Jafari [22]. Accordingly to the Coulomb friction criteria, both the initial and residual shear properties (shear strength and friction coefficient) were evaluated. Additionally, from each shear stress versus sliding displacement curve, the mode-II fracture energy was evaluated excluding the energy dissipated due to the friction [9].

2.4. Testing procedures for determining flexural bond properties

The flexural bond strength at brick–mortar interfaces was determined with an advanced bond wrench set-up as proposed by Gaggero and Esposito [37], which complies also with the standard EN 1052–5 [38]. This allows determining both the flexural bond strength as well as the bond fracture energy. This set-up enables to control the crack mouth opening displacement (CMOD) at the tension side of the couplet (Fig. 2 (d)). A 250 kN hydraulic jack was employed to apply the vertical load at the free end of the level arm, while the two LVDTs (measuring range + 2 mm) positioned between the upper and lower clamps was used to control the test at a rate of 0.001 mm/s. Besides, another two LVDTs were glued between the top and bottom bricks at the left and right side to acquire an accurate measurement of the crack mouth opening displacement at the mortar joint.

The flexural bending stress of couplets was calculated, in accordance with the EN 1052–5 [38] with the following formula:

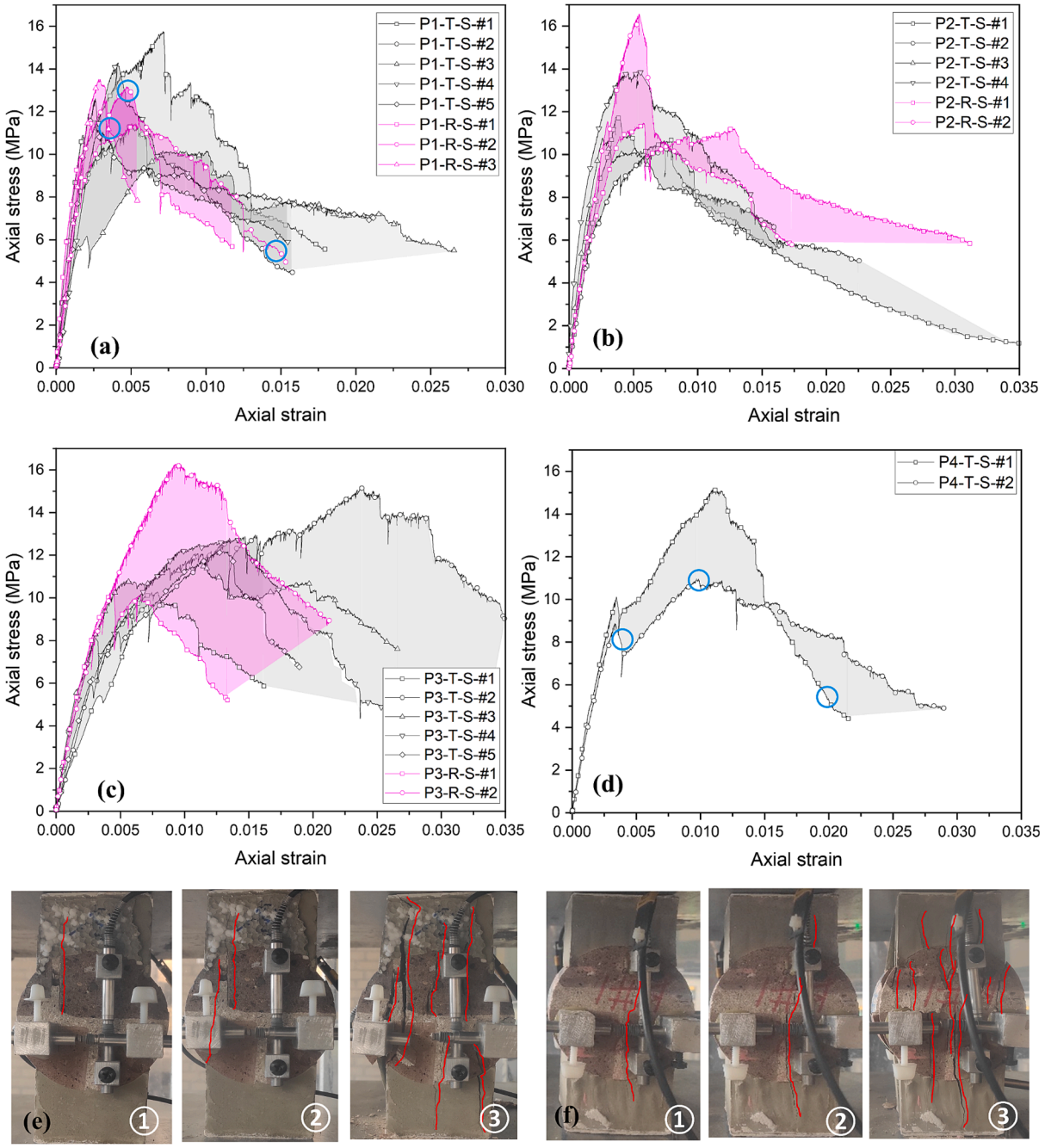

Fig. 3. Axial stress versus axial strain under compression for single-wythe cores extracted from: P1(a), P2(b), P3(c) and P4(d); the evolution of crack pattern for core P1-R-S-#2 (e) and P4-T-S-#2 (f).

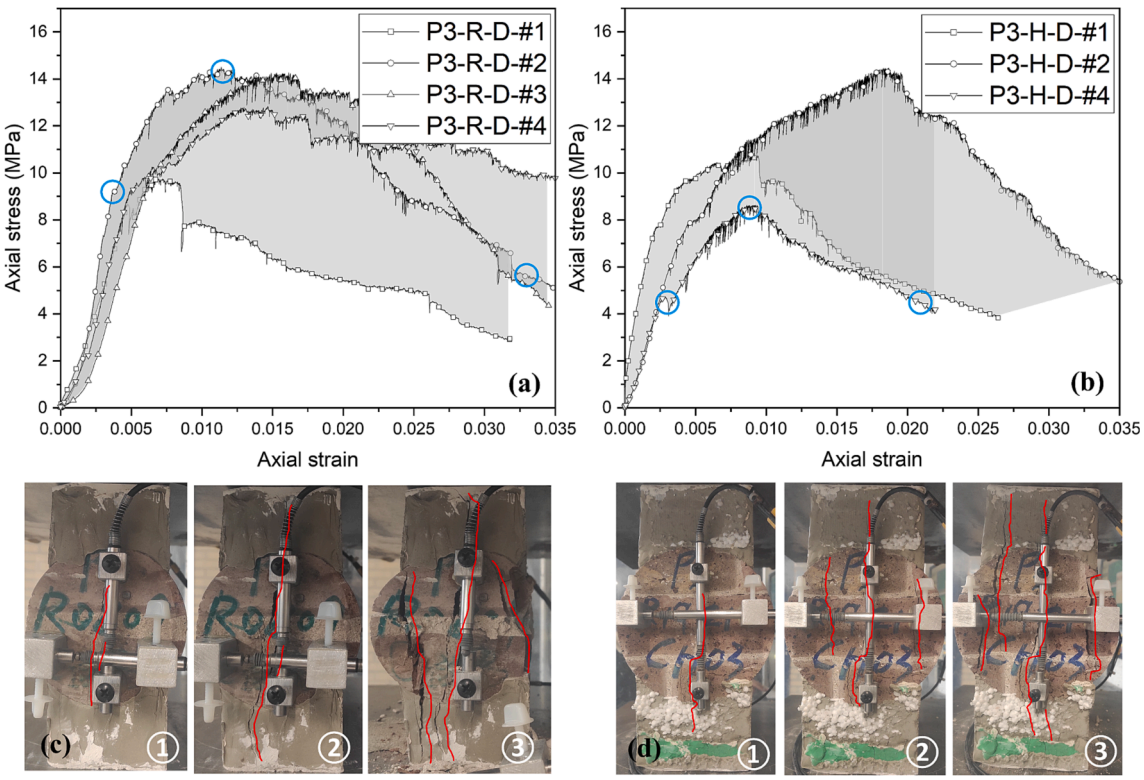

Fig. 4. Axial stress versus axial strain under compression for double-wythe cores extracted from P3 with the random bond pattern (a) and the H-shaped bond pattern (b); the evolution of crack pattern for core P3-R-D-#2 (c) and P3-H-D-#4 (d).

$$f_w = \frac{F_1 e_1 + F_2 e_2 - \frac{2}{3} d\left(F_1 + F_2 + \frac{W}{4}\right)}{\frac{bd^2}{6}} \quad (3)$$

where F_1 is the load from the testing machine, F_2 (85.85 N) is the normal force as a result of the weight of the bond wrench apparatus, W is the weight of the masonry brick pulled off the specimen and any adherent mortar, e_1 (460 mm) is the distance from the applied load to the tension face of the specimen, e_2 (53.1 mm) is the distance from the centre of gravity of the clamp to the tension face of the specimen, b and d is the mean length of the bed joint and the mean width of the bed joint respectively. Based on the area underneath the curve of force and vertical displacement of jack [37], the bond fracture energy can also be evaluated, by assuming that the energy dissipation due to the joint cracking is the same as the work of the testing machine.

3. Results

The global stress–strain/displacement relationship of cores and rectangular samples under different loading conditions are presented in this section, together with the crack pattern and failure mode of samples involved. It can serve for evaluating compressive properties of masonry, shear properties and flexural bond properties at brick–mortar interfaces showed in Section 4.

3.1. Compressive properties of masonry

The overall response of all specimens subjected to compressive load is analysed in terms of stress–strain relationship and crack pattern evolution. The evolution of crack pattern is presented for each type of

Table 4
Average compressive strength of single-wythe cores from P1-P4.

Group ID	Wall portion	Bond pattern	Number of samples	Compressive strength (MPa)	C.o.V. (%)
P1-T-S	P1	T	5	12.85	17.32
P1-R-S		R	3	12.72	8.69
P2-T-S	P2	T	4	11.71	13.39
P2-R-S*		R	2	14.02	25.69
P3-T-S	P3	T	5	12.52	14.16
P3-R-S*		R	2	13.35	30.92
P4-T-S*	P4	T	2	13.09	22.86

Table 5
Average compressive strength of double-wythe cores from P3.

Group ID	Wall portion	Bond pattern	Number of samples	Compressive strength (MPa)	C.o.V. (%)
P3-R-D	P3	R	5	12.52	16.07
P3-H-D		H	4	11.54	21.32

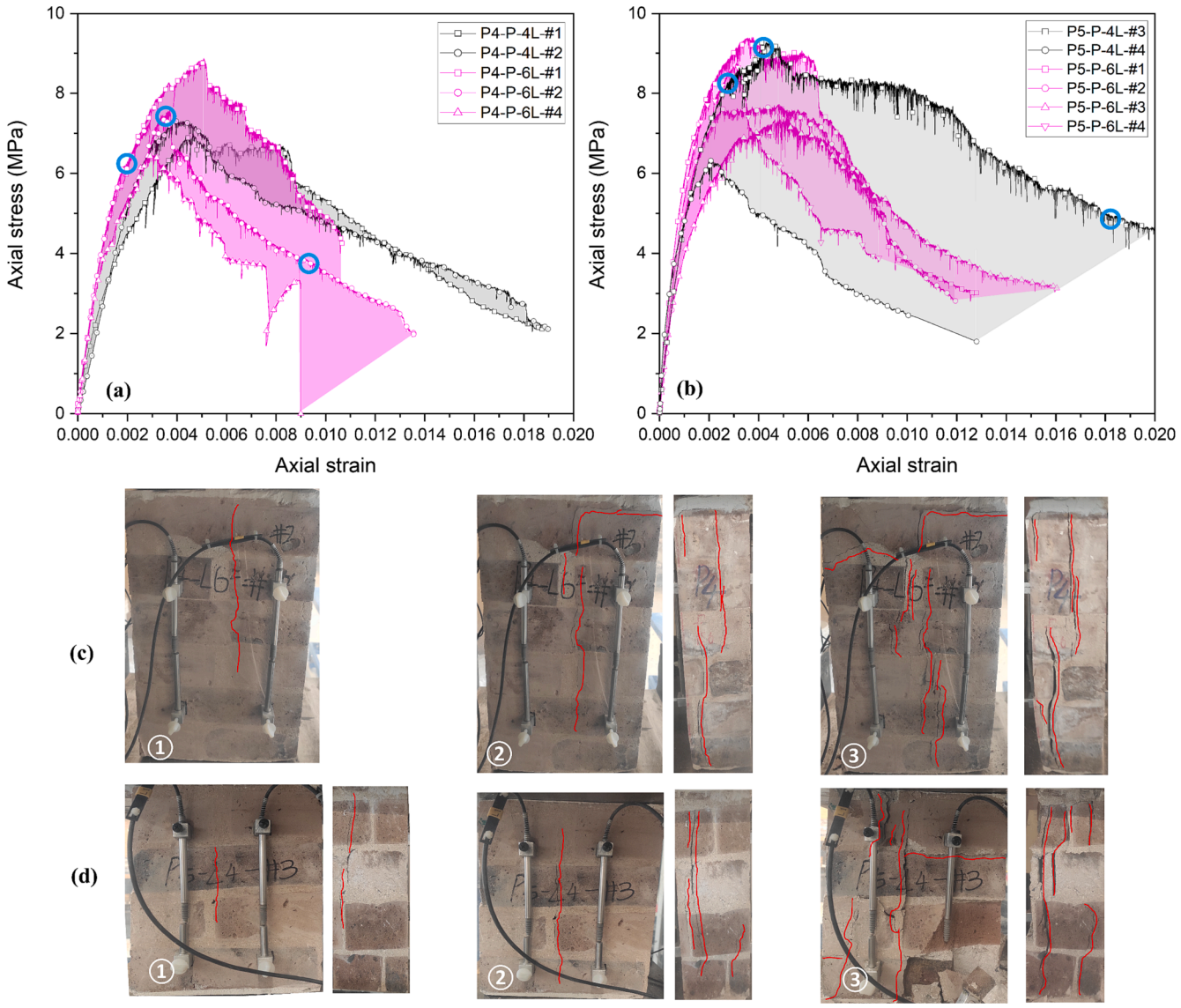

Fig. 5. Axial stress versus axial strain under compression for 4-layer and 6-layer prisms extracted from P4(a) and P5(b); the evolution of rack pattern for the prism P4-P-6L-#2(c) and P5-P-4L-#3(d).

Table 6
Average compressive strength of prisms from P4 and P5.

Group ID	Wall portion	Number of brick layers	Number of samples	Compressive strength (MPa)	C.o.V. (%)
P4-P-4L	P4	4	3	6.89	8.10
P4-P-6L		6	4	7.53	13.25
P5-P-4L	P5	4	4	7.45	17.12
P5-P-6L		6	4	8.32	11.17

cores and prisms considering the following phases: onset of cracking (①), peak force (②) and failure (③). In section 4, the compressive properties in terms of elastic modulus, compressive strength, compressive fracture energy and strain at peak are presented.

3.1.1. Cores

Fig. 3 and Fig. 4 plots the scattering region of the stress–strain response for single-wythe and double-wythe cores under compression, as well as the evolution of crack pattern. For all types of cores, the stress–strain response under compression starts from a linear-elastic stage, then followed by an pre-peak softening behaviour until the peak stress. This pre-peak softening stage usually initiates at the first reduction of force during the testing, at which moment the crack occurred suddenly along the head joint of the cores and propagated to the cap. With the increase of the axial strain, the crack opened perpendicular to the loading direction and propagated vertically. After reaching the peak stress, both nonlinear and linear softening behaviour can be observed for different samples, and multiple cracks generated broadly and led to the final collapse. It can be observed that the slope of the stress–strain curves in the linear-elastic stage is steeper for samples from P1 and P2 (external), than those from P3 and P4 (internal). Subsequently, a lower strain at peak is recorded for cores from P1 and P2, in comparison with

cores from P3 and P4. Table 4 and Table 5 list the compressive strength of single-wythe cores and double-wythe cores. It should be noted that the premature failure of the cap was undesired, but it could not be associated to any geometrical imperfection. Considering the rapid recovery of stresses after onset of cracking, it can be considered that this premature failure has a negligible influence on the compressive strength and strain at peak; on the other hand results associated to the fracture energy should be taken with care. Overall, the identification of a better capping material is needed to eliminate the premature failure of cores under compression, so that both pre- and post- peak behaviour can be accurately estimated.

3.1.2. Prisms

Fig. 5 plots the scattering region of the stress–strain response for prisms with 4-layer bricks (black lines) and 6-layer bricks (magenta lines) under compression and the evolution of crack pattern. A similar trend to the core can be observed. From the front view of the prism, a vertical crack initiated suddenly along the head joint and across the bricks during the pre-peak softening phase of the stress–strain response, which could also occur at the lateral surface. Subsequently, this crack will propagate vertically and other cracks along the head joint or the bed joint could further accumulate until reaching the peak force. At the post-peak phase, the sample gradually lost the load-bearing abilities due to the extensive cracks accompanied by large crack opening perpendicular to the loading direction. Besides, the slope of the stress–strain curves in the linear-elastic stage is steeper for samples from P5 (external), than those from P4 (internal), which is in consistence with the findings from cores. In order to obtain rectified samples, the height-to-thickness ratio in the present work ranges from 3.16 to 3.98 for the 6-layer prism, while the scatter is from 2.05 to 3.18 for the 4-layer prism. Although the height-to-thickness ratio of the 6-layer prism is averagely larger than that of the 4-layer prism, the compressive strength is similar among two types of samples as listed in Table 6, which is different from what reported by Thaickavil and Thomas [39] (Fig. 5 and Fig. 12). This phenomenon could be attributed to the scatter of length-to-thickness ratio among samples, which varies from 1.78 to 3.07. Absai et al. [40] found that the compressive strength of masonry is considerably affected by the length-to-thickness ratio, especially in short prisms. Therefore, it is possible that both the effect of the length-to-thickness ratio and the effect of height-to-thickness ratio coupled together, contributing to the similar compressive strength across 4-layer and 6-layer prisms in the current study.

3.2. Shear properties of brick–mortar interfaces

In this section, shear properties at brick–mortar interfaces, i.e. initial shear strength (or cohesion), coefficient of friction and mode-II fracture energy, are presented for both splitting tests on I-shaped cores and shear-compression tests on triplets. Due to the large presence of header bond pattern in the cut pieces, extraction of triplets was possible only from P2.

3.2.1. Cores

Fig. 6 shows the shear stress versus the sliding displacement measured between the two portions of bricks, where a significant scatter

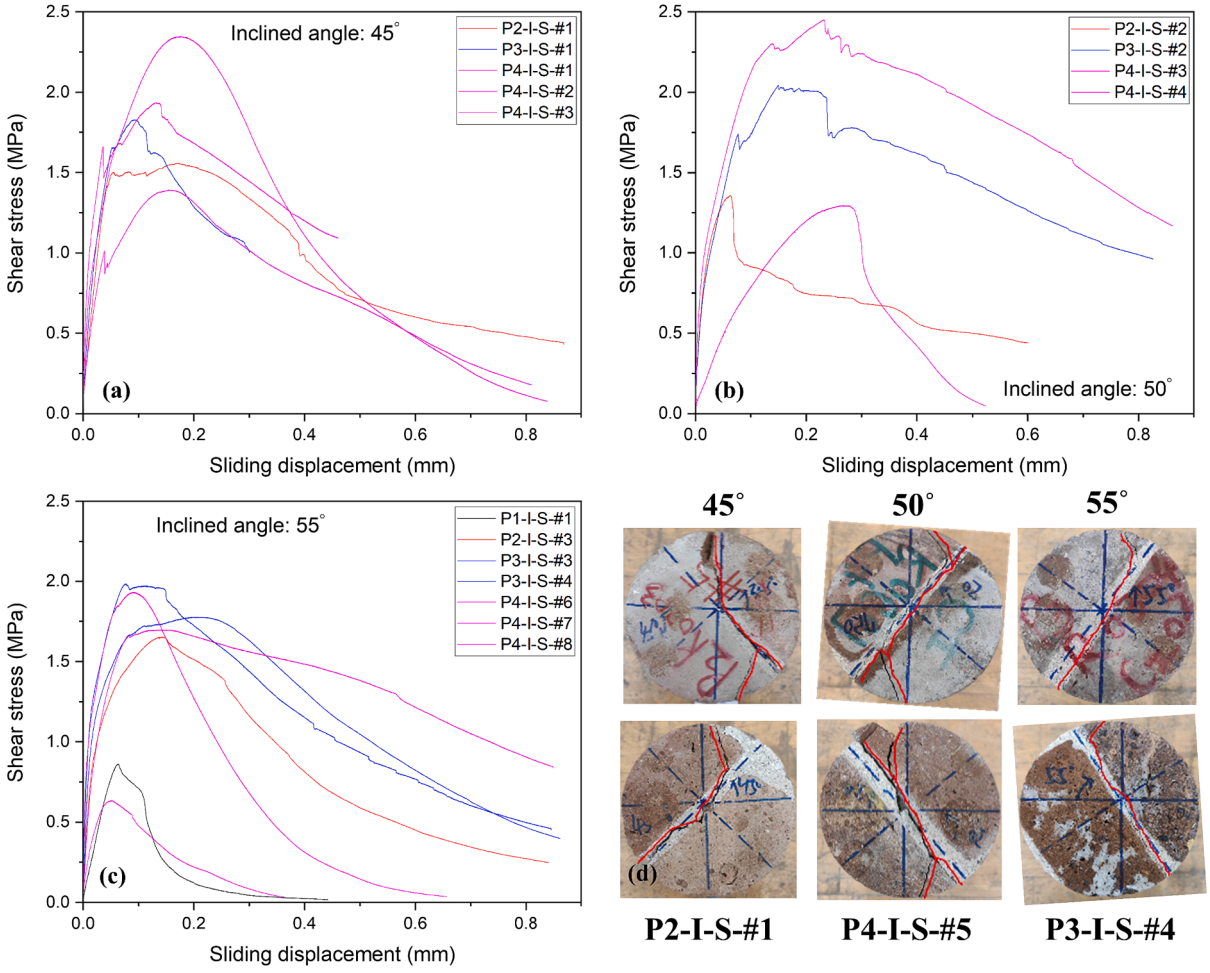

Fig. 6. Stress-sliding relationship observed during shear tests on the I-shaped cores with the inclined angle: (a) 45°; (b) 50°; (c) 55°; (d) failure modes for each inclined angle.

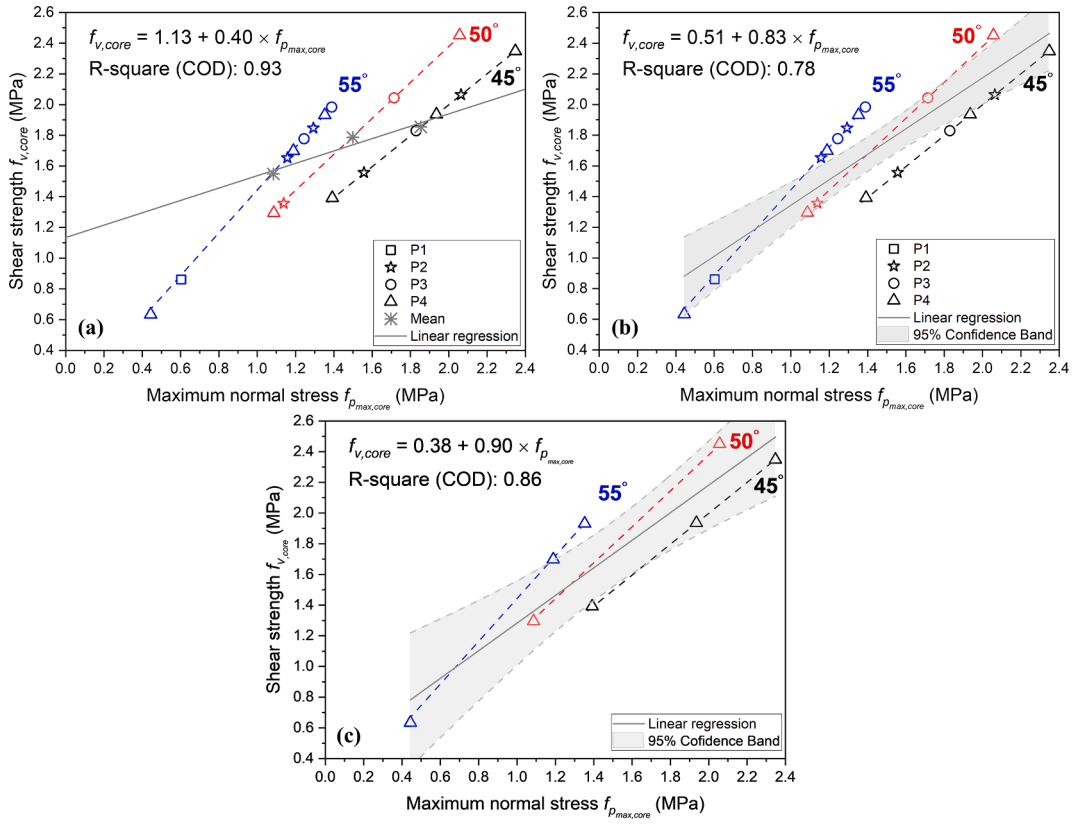

Fig. 7. Failure envelope from splitting tests on cores using: (a) the average result for each inclination; (b) all data from P1 to P4; (c) all data from P4.

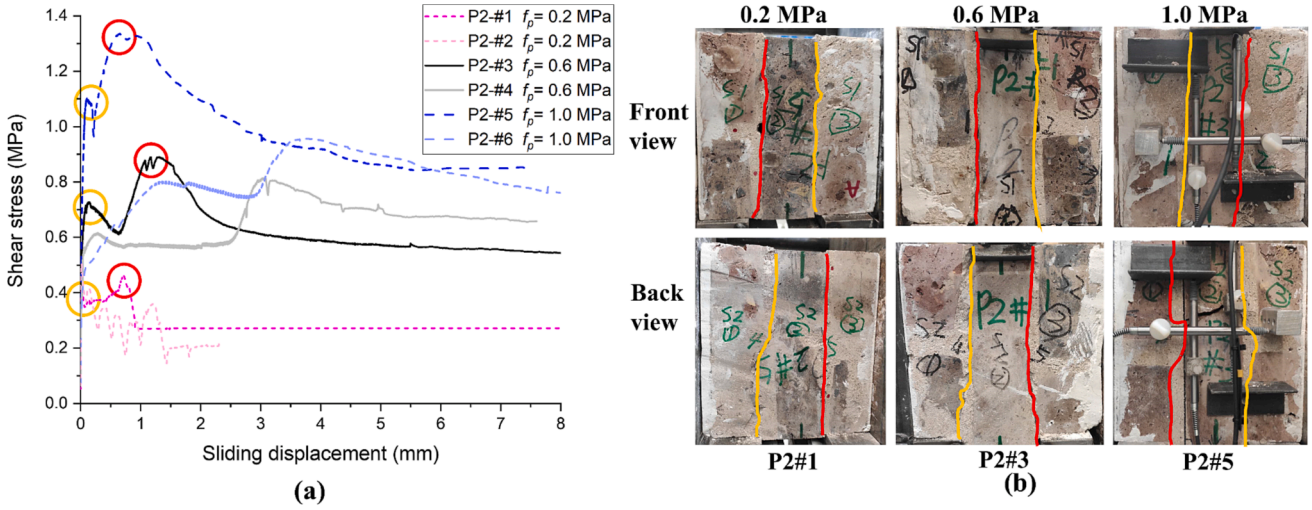

Fig. 8. Shear stress versus sliding displacement for triplets at different pre-compression loads (a); crack pattern at brick–mortar interfaces at the final failure (b).

can be observed among samples for each inclined angle. In most cases, a mixed failure involving both tensile failure of the bricks and sliding at brick–mortar interfaces occurred (Fig. 6(d)); in few cases, a pure tensile splitting failure of the core occurred. Therefore, the scatter in Fig. 6 (a)-(c) can be partially associated to different mixing between tensile failure of bricks and sliding failure at interfaces. In the realm of computing the shear properties at the interface, only the specimens failing under mixed tensile-sliding failure were considered.

Fig. 7 shows the failure envelope in terms of shear stress versus compression stress relationship for all the results obtained from P1 to P4. Considering the regression analysis with the average results for each inclination [12], an initial shear strength $f_{v0,core}$ of 1.13 MPa and coefficient of friction μ of 0.40 are obtained (Fig. 7(a)); however, these results are unconventional considering typical values for brick masonry [9,12,13]. Regarding the regression analysis of all results [13], an initial shear strength $f_{v0,core}$ of 0.51 MPa and coefficient of friction μ of 0.83 are obtained (Fig. 7(b)), which are within the scatter range of what is reported in literature [9,12,13]. In view of the large scatter of the results, the latter method seems to be more appropriate for this case study. Although the mode-II fracture energy of the brick–mortar interface can be obtained from core testing, by removing the friction contribution from the total dissipated energy, as proposed by Jafari et al. [9], it is hard to separate the fracture energy dissipated at bricks from that dissipated at interfaces for the present study. Therefore, the fracture

Table 7
Shear strength evaluated at the first peak, shear strength evaluated at the second peak, residual shear strength and mode-II fracture energy for each specimen.

Specimen name	f_p(MPa)	f_v^I(MPa)	f_v^{II}(MPa)	$f_{v,res}$(MPa)			$G_{f\text{-}II}$ (N/mm)
				f_p = 0.2 MPa	f_p = 0.6 MPa	f_p = 1.0 MPa	
P2-#1	0.2	0.82	0.46	0.27	0.60	0.90	0.11
P2-#2	0.2	1.00	–	0.21	0.51	0.79	–
P2-#3	0.6	0.73	0.89	–	0.54	–	0.69
P2-#4	0.6	1.23	0.82	–	0.57	–	–
P2-#5	1.0	2.20	1.34	0.19	0.49	0.85	0.99
P2-#6	1.0	1.60	0.96	–	–	–	–

Note: - denotes values that are not available or excluded for the calculation of shear properties in Fig. 9.

energy from splitting tests on cores was not evaluated here due to the mixed tensile-shear failure mode of cores.

Arguing that the large scatter of the results could be influenced by variation on the properties through the thickness of the wall, a regression analysis for cores extracted from P4 (internal) was also performed having for this piece the largest number of specimens. In this case, an initial shear strength $f_{v0,core}$ of 0.38 MPa and coefficient of friction μ of 0.90 are obtained (Fig. 7(c)).

3.2.2. Triplets

Fig. 8 shows the shear stress versus sliding displacement along the brick–mortar interfaces during the shear-compression tests on triplets. For the majority of the specimens, two peaks in shear stress were observed before reaching the plateau, regardless of the pre-compression stress level. Similar findings have been reported by Segura et al. [41]. This behaviour is the result of a non-simultaneous failure of the two brick–mortar interfaces; in fact the first peak is associated with cracking at one brick–mortar interface, while the second peak marks the failure of the other brick–mortar interface. The sequential cracking of the two interfaces might be attributed to the slight unevenness of the contact surface between the middle brick and the load cell, which was difficult to eliminate during the extraction process. Another possible reason is that the two interfaces exhibited different properties due to the presence of defects, e.g. for sample P2-#1 a hole is found on the left interface (Fig. 8(b)).

Few exception were found for some specimens that led to the exclusion of some data in the calculation of the shear properties. Despite the effort in rectifying the specimens, out-of-plane rotation of the middle brick were observed after the second peak for the specimen P2-#6. Specimen P2#2 showed significant fluctuation of the pre-compression stress (20 %-50 %) in correspondence of the cracking of the second interface (after the first peak, but before reaching the plateau). Consequently, residual properties were not calculated for specimen P2-#6 and initial shear properties associated to the second peak were not considered for specimen P2-#2 (Table 7). Additionally, cracking of the middle

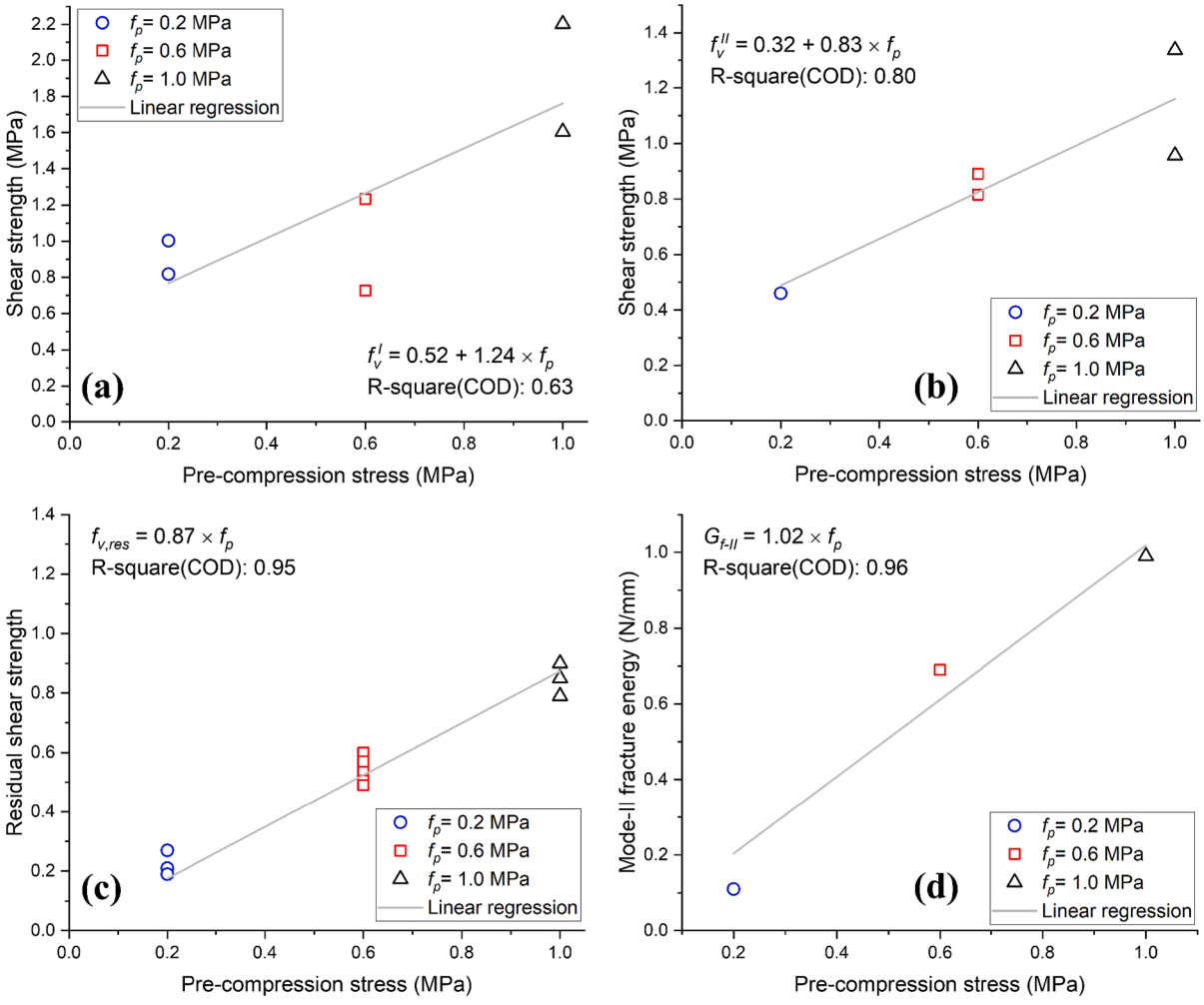

Fig. 9. Shear strength evaluated at the first peak (a), shear strength evaluated at the second peak (b), residual shear strength (c) and mode-II fracture energy (d) as a function of pre-compression stress.

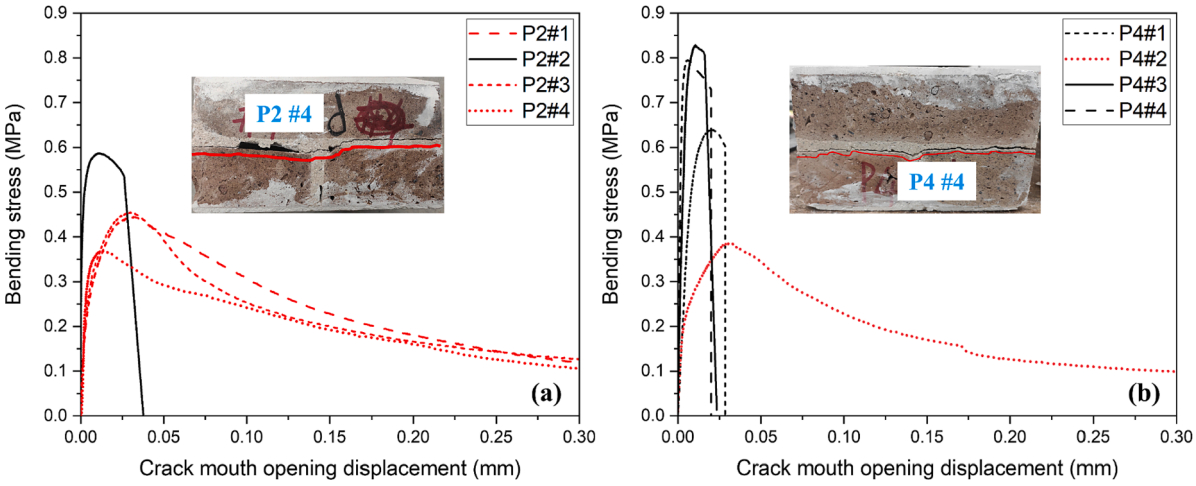

Fig. 10. Bending stress at the brick–mortar interfaces with the increase of crack mouth opening displacement for couplets extracted from P2 (a) and P4 (b).

brick for specimen P2-#5 was observed after the second peak, which may indicate the presence of out-of-plane deformation.

The initial shear properties were evaluated considering both the strength related to the first peak f_v^I and the strength related to the second peak f_v^{II}. In the first case, the initial shear strength $f_{v,0}^I$ and the friction coefficient μ^I are found equal to 0.52 MPa and 1.24, respectively. (Fig. 9 (a)). In the second case, the initial shear strength $f_{v,0}^{II}$ and the friction coefficient μ^{II} are found equal to 0.32 MPa and 0.83, respectively (Fig. 9 (b)). For the present study, it is recommended to evaluate the shear properties considering the results associated to the second peak in shear stress. This is because the results associated with the first peak provide relatively large values for friction coefficient that are not representative for masonry. Additionally, considering that different properties are obtained for the two cases, it may be argue that the second interface would present minor cracks at the first peak that are not considered in the calculation of f_v^I. A residual friction coefficient equal to 0.87 is obtained (Fig. 9(c)). A mode-II fracture energy ranging between 0.1 N/mm and 1.0 N/mm is obtained considering the specimens P2-#1, P2-#3 and P2-#5 (Fig. 9(d) and Table 7).

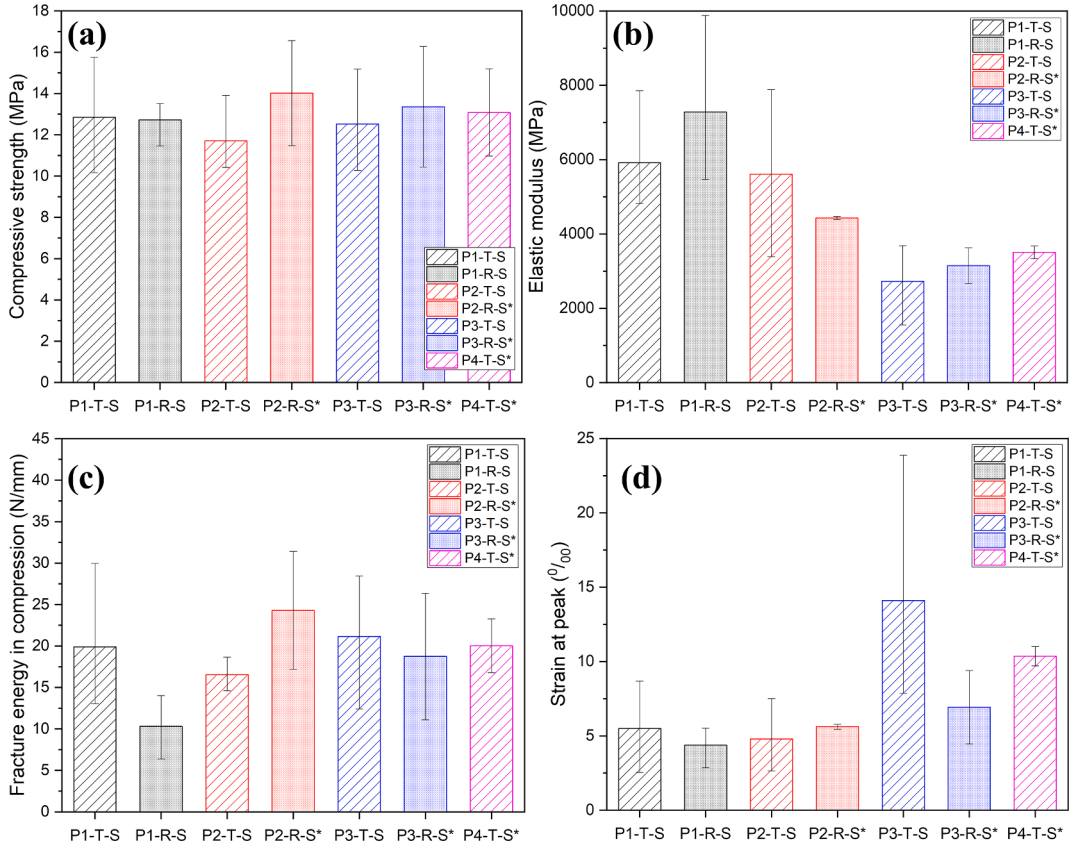

Fig. 11. Mean values of compressive strength (a), elastic modulus (b), fracture energy in compression (c) and strain at peak, (d) for single-wythe cores extracted from P1 to P4.

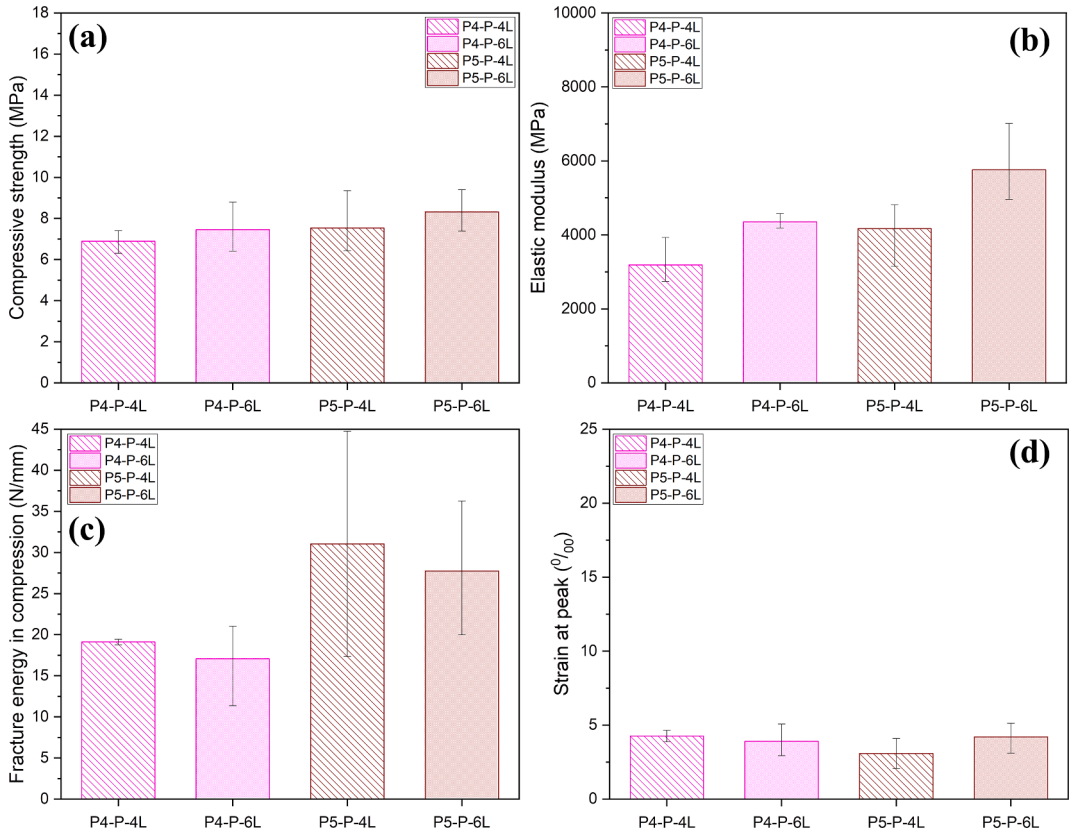

Fig. 12. Mean values of compressive strength (a), elastic modulus (b), fracture energy in compression (c) and strain at peak (d) for prims extracted from P4 and P5.

3.3. Flexural properties of brick–mortar interfaces

Two types of failure mode were observed for couplets: a brittle failure and a quasi-brittle failure (Fig. 10). The brittle failure mode behaves as sudden cracking at the brick–mortar interface accompanied with the sudden drop of the force from load cell (black lines in Fig. 10); the quasi-brittle failure mode acts as the progressive crack propagation at interfaces along with the post-peak softening (red lines in Fig. 10). The majority of the specimens from P2 (external) showed a quasi-brittle failure mode, while brittle failure occurs more frequently for couplets from P4 (internal). Regarding the crack pattern as showed in Fig. 10, the migration of crack from one brick–mortar interface to the other was observed from the front view for almost all specimens, except for one specimen from P4 with the crack surface located at a single brick–mortar interface. The predominant failure mechanism (quasi-brittle failure for P2 and brittle failure for P4) was considered to calculate the bond properties (Fig. 13). It should be noted that this leads to a very low coefficient of variation (within 30 %), which is quite rare for masonry [22].

4. Discussions

In this section, the compressive properties, shear properties and flexural bond properties of the masonry wall changing through the thickness direction are discussed, while the correlation of compressive and shear properties obtained from cores and rectangular samples is explored for further validating the slightly-destructive core testing method.

4.1. Through thickness effect

A through-thickness effect is not observed for all the mechanical properties, but it is recorded only for the elastic modulus, strain at peak, fracture energy under compression, flexural bond strength and bond fracture energy.

Fig. 11 and Fig. 12 shows the compressive properties for different pieces as obtained with T-shaped and R-shaped single-wythe cores, and prisms, respectively. The compressive strength does not show a through-thickness effect; conversely the elastic modulus is lower for the internal masonry piece (P3 and P4) than the external masonry piece (P1, P2, P5). The results between cores and prisms are consistent, except for the case of the compressive fracture energy and strain at peak. For cores, no through-thickness effect for compressive fracture energy is observed, while for prisms it is found a higher value for external masonry piece (P5) with respect to internal masonry piece (P4). Regarding strain at peak, it is higher for the internal masonry piece (P3 and P4) than the external masonry piece (P1, P2, P5) for cores, while no through-thickness-effect can be observed for prisms.

As for the shear properties, no clear trend about the through-thickness effect can be identified due to the large scatter of the data (see Fig. 6).

Regarding the flexural bond properties, the bond strength and bond fracture energy are higher in the internal piece P4, compared with that from external piece P2 (Fig. 13(a)); this implies that the masonry has weaker bond properties in the portion closer to the water. Further, precipitated material on the failure surface was observed (Fig. 13(b)-(c)). This precipitated material is extended over a large area for most of couplets from P2 (external), while it is localised in small spots for couplets from P4 (internal); this could indicate the presence of degradation mechanisms. Despite the through-thickness effect, the bond properties are generally higher and show a lower coefficient of variation than the properties obtained for clay brick masonry specimens extracted from Dutch housing buildings in the Groningen region without underwater construction [22,37,42,43].

The cause of the through-thickness-effect may be multiple, but the authors suspect that this is the results of a degradation/aging

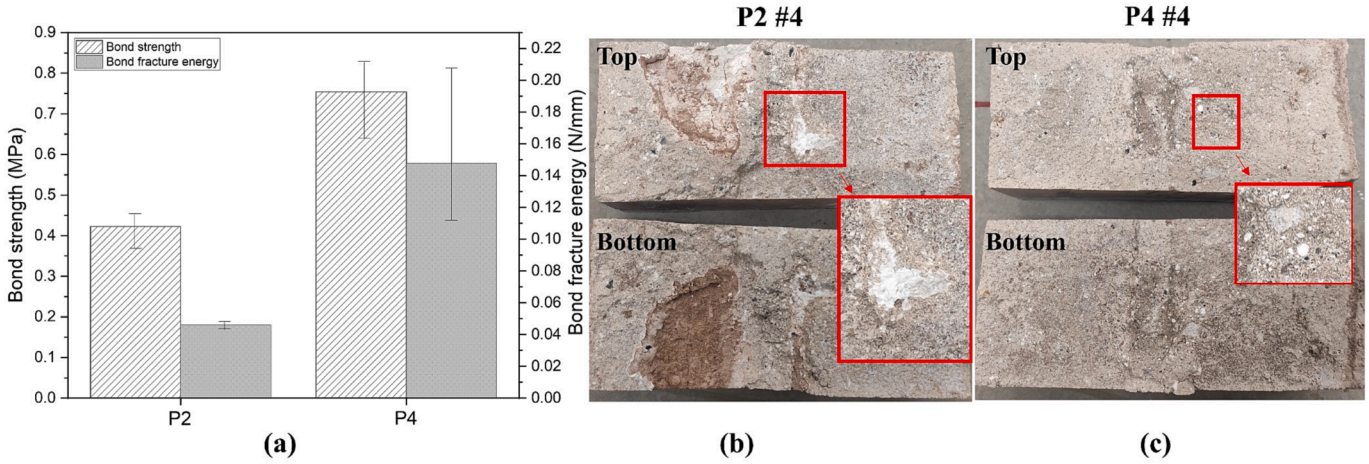

Fig. 13. Mean values of bond strength and bond fracture energy for couplets extracted from P2 and P4 (a); Crack surface of the sample from P2 (b); Crack surface of the sample from P4 (c).

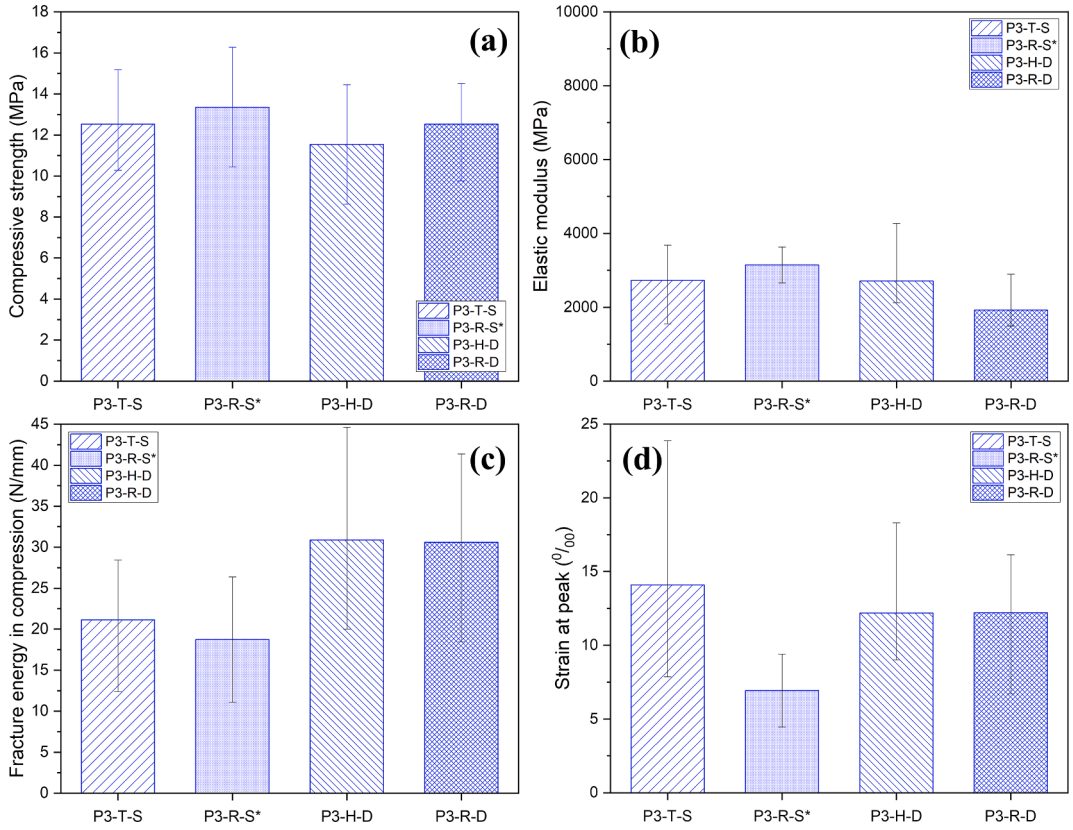

Fig. 14. Mean values of compressive strength (a), elastic modulus (b), fracture energy in compression (c) and strain at peak (d) for single-wythe and double-wythe cores extracted from P3.

mechanism. The precipitated material noticed in couplets may be a sign of the chemical reaction at the mortar joints with the exposure to intensive humidity. Nijland et al. [44] mentioned that mortars could develop a range of reactions in the formation of the secondary phases, such as ettringite, thaumasite and gypsum, with the presence of water as a transport agent and a reacting compound. These newly-formed secondary phases could occasionally fill part of air voids and result in cracking when empty space is not enough. Besides, self-healing of mortars may be active along with the precipitation of Ca-carbonate [45], which could fill in cracks or voids at one location, and generate new porosity at other locations [44]. Such phenomena will explain the presence of precipitated material within the pore to be larger in the external masonry pieces than the internal ones. Additionally, the fact that no difference in brick properties are found through the thickness (Table 1), supports that both the internal and external masonry piece are of the same masonry typology. Another possible cause or concurring cause could be the uneven load distribution of the pillar, leading to a different loading history for the internal and external part of the pillar. Further studies at the micro-level are needed to identify the presence of deterioration mechanisms or other concurring causes to the through-thickness effect of mechanical properties.

4.2. Benchmarking the core testing method

Fig. 14 presents the compressive properties of different type of cores extracted from P3. In the current study, bond patterns (i.e. T-shaped, R-shaped, H-shaped) and dimensions of cores have a negligible effect on compressive properties. However, more research on different masonry typologies is required to obtain a sound conclusion in this respect, considering that in literature a decrease of the masonry compressive strength is showed with the presence of head joints in masonry cores [19]. The similarities of compressive properties from different types of cores could alleviate difficulties of in-field core extraction, especially for multi-wythe masonry structures with a priori unknown bond patterns along the thickness.

Compared with results obtained from rectangular specimens, the results obtained with core testing show some differences. Similar elastic modulus and fracture energy under compression are shown for cores and prisms both from P4, whereas the compressive strength and strain at peak from cores are approximately two times larger than the ones from prisms (Fig. 11 and Fig. 12). For splitting tests on I-shaped cores from P1 to P4, the initial shear strength is about 1.55 times larger than that from triplets (calculated considering the second peak of the shear stress), while the friction coefficient is the same, 0.83. When considering only cores from P4 (highest number of samples for splitting tests on cores), the initial shear strength (i.e. 0.38 MPa) is very closed with the one from triplets (i.e. 0.32 MPa).

5. Conclusions

Based on the analysis of tests on cores and rectangular specimens extracted above water level from a bridge pillar built in 1882 in Amsterdam, the present work provides preliminary conclusions for the characterization of multi-wythe brick masonry infrastructure:

- Due to the difficulties of extracting rectangular samples from multi-wythe brick masonry infrastructure, the core testing method seems to be one of the most efficient slightly-destructive test to be employed for characterization of mechanical properties. Additionally, this gives the advantage that in case of composite structures, i.e. masonry/reinforced - concrete walls or presence of renovation, the same sample can be adopted independently of the construction material.
- Bond patterns and dimensions of cores have negligible effect on compressive properties; however, this needs to be extensively verified by considering other masonry typologies.
- Due to significant scatter of test data from the splitting tests on cores, for the calculation of shear properties (i.e. initial shear strength and coefficient of friction) the regression line approximating all the data is more reliable than that the one approximating the average of each inclination. Nevertheless, further investigations are needed to evaluate the role of brick failure in the mixed tensile-sliding failure mode.
- For this case study, a through-thickness effect for some compressive properties (elastic modulus and strain at peak) and for the bond properties (flexural bond strength and bond fracture energy) could be identified: the compressive behaviour of the masonry is stiffer and the flexural bond properties are weaker when being closer to water. However, it was not possible to identify a clear trend for the shear properties due to the limited data with a high coefficient of variation. Further investigations at the micro-level would be suggested for exploring the causes of the through-thickness effect.
- Further improvement to the core testing method to assess the mechanical properties of multi-wythe brick masonry is required. Among others, the following aspects are identified: the study of specimen size and bond pattern on the compressive behaviour, the identification of a better capping material for the estimation of both pre- and post- peak behaviour, the improvement of splitting tests on core to obtain solely failure at the brick–mortar interface in the case of high bond properties.

Overall, the present work shows the basis for the definition of a material characterisation strategy for multi-wythe brick masonry, which is limited in literature, and will support the assessment of many infrastructure in typical Dutch canal cities.

Declaration of Competing Interest

The authors declare that they have no known competing financial interests or personal relationships that could have appeared to influence the work reported in this paper.

Data availability

The experimental results of the presented tests are available via the 4TU.ResearchData repository (https://doi.org/10.4121/67b48e11-9b86-40a5-802d-8e2dcd16eaea. The data will be distributed under the license type CC BY.

Acknowledgement

This research was funded by the municipality of Amsterdam via the Amsterdam institute for Advanced Metropolitan Solutions (AMS) within the scope of the research programme Bridges and Quay Walls (Programma Bruggen en Kademuren). The authors would like to acknowledge the support of PhD student Maria Belen Gaggero for knowledge transfer on experimental set-ups and the technical staff of Macrolab/Stevinlaboratory at Faculty of Civil Engineering and Geosciences, TU Delft.

References

[1] Kademuren, maatregelen en vernieuwen, (2022). https://www.amsterdam.nl/projecten/kademuren/.
[2] M. Korff, M. Hemel, R. Esposito, Bezwijken Grimburgwal: Leerpunten voor het Amsterdamse areaal, Delft, The Netherlands, 2021.
[3] N. Domede, A. Sellier, T. Stablon, Structural analysis of a multi-span railway masonry bridge combining in situ observations, laboratory tests and damage modelling, Eng. Struct. 56 (2013) 837–849, https://doi.org/10.1016/j.engstruct.2013.05.052.
[4] S. Sharma, M. Longo, F. Messali, A novel tier-based numerical analysis procedure for the structural assessment of masonry quay walls under traffic loads, Front. Built Enviroment. 9 (2023) 1–17, https://doi.org/10.3389/fbuil.2023.1194658.
[5] I. Roselli, M. Malena, M. Mongelli, N. Cavalagli, M. Gioffrè, G. De Canio, G. de Felice, Health assessment and ambient vibration testing of the "Ponte delle Torri" of Spoleto during the 2016–2017 Central Italy seismic sequence, J. Civ. Struct. Heal. Monit. 8 (2018) 199–216, https://doi.org/10.1007/s13349-018-0268-5.
[6] P. Borlenghi, A. Saisi, C. Gentile, ND testing and establishing models of a multi-span masonry arch bridge, J. Civ. Struct. Heal. Monit. (2023), https://doi.org/10.1007/s13349-022-00666-1.
[7] E. Alpaslan, M.F. Yilmaz, B.D. Şengönül, Rating and reliability assessment of a historical masonry arch bridge, J. Civ. Struct. Heal. Monit. (2023), https://doi.org/10.1007/s13349-023-00692-7.
[8] L. Pelà, E. Canella, A. Aprile, P. Roca, Compression test of masonry core samples extracted from existing brickwork, Constr. Build. Mater. 119 (2016) 230–240, https://doi.org/10.1016/j.conbuildmat.2016.05.057.
[9] S. Jafari, J.G. Rots, R. Esposito, Core testing method to assess nonlinear shear-sliding behaviour of brick-mortar interfaces: A comparative experimental study, Constr. Build. Mater. 244 (2020) 118236, https://doi.org/10.1016/j.conbuildmat.2020.118236.
[10] S. Jafari, J.G. Rots, R. Esposito, Core testing method to assess nonlinear behavior of brick masonry under compression: A comparative experimental study, Constr. Build. Mater. 218 (2019) 193–205, https://doi.org/10.1016/j.conbuildmat.2019.04.188.
[11] F. Ferretti, B. Ferracuti, C. Mazzotti, M. Savoia, Destructive and minor destructive tests on masonry buildings: Experimental results and comparison between shear failure criteria, Constr. Build. Mater. 199 (2019) 12–29, https://doi.org/10.1016/j.conbuildmat.2018.11.246.
[12] C. Mazzotti, E. Sassoni, G. Pagliai, Determination of shear strength of historic masonries by moderately destructive testing of masonry cores, Constr. Build. Mater. 54 (2014) 421–431, https://doi.org/10.1016/j.conbuildmat.2013.12.039.
[13] L. Pelà, K. Kasioumi, P. Roca, Experimental evaluation of the shear strength of aerial lime mortar brickwork by standard tests on triplets and non-standard tests on

core samples, Eng. Struct. 136 (2017) 441–453, https://doi.org/10.1016/j.engstruct.2017.01.028.
[14] D. Marastoni, L. Pelà, A. Benedetti, P. Roca, Combining Brazilian tests on masonry cores and double punch tests for the mechanical characterization of historical mortars, Constr. Build. Mater. 112 (2016) 112–127, https://doi.org/10.1016/j.conbuildmat.2016.02.168.
[15] J. Segura, L. Pelà, P. Roca, A. Cabané, Experimental analysis of the size effect on the compressive behaviour of cylindrical samples core-drilled from existing brick masonry, Constr. Build. Mater. 228 (2019), 116759, https://doi.org/10.1016/j.conbuildmat.2019.116759.
[16] International Union of Railways(UIC) UIC code 778-3R, Recommendations for the assessment of the load carrying capacity of existing masonry and mass-concrete arch bridges, 1995.
[17] A. Brencich, D. Sabia, Experimental identification of a multi-span masonry bridge: The Tanaro Bridge, Constr. Build. Mater. 22 (2008) 2087–2099, https://doi.org/10.1016/j.conbuildmat.2007.07.031.
[18] E. Sassoni, C. Mazzotti, The use of small diameter cores for assessing the compressive strength of clay brick masonries, J. Cult. Herit. 14 (2013) e95–e101, https://doi.org/10.1016/j.culher.2012.11.027.
[19] J. Dorji, T. Zahra, D. Thambiratnam, D. Lee, Strength assessment of old masonry arch bridges through moderate destructive testing methods, Constr. Build. Mater. 278 (2021), 122391, https://doi.org/10.1016/j.conbuildmat.2021.122391.
[20] E. Sassoni, C. Mazzotti, G. Pagliai, Comparison between experimental methods for evaluating the compressive strength of existing masonry buildings, Constr. Build. Mater. 68 (2014) 206–219, https://doi.org/10.1016/j.conbuildmat.2014.06.070.
[21] M. Ispir, C. Demir, A. Ilki, N. Kumbasar, Material Characterization of the Historical Unreinforced Masonry Akaretler Row Houses in Istanbul, J. Mater. Civ. Eng. 22 (2010) 702–713, https://doi.org/10.1061/(asce)mt.1943-5533.0000071.
[22] S. Jafari, Material characterisation of existing masonry A strategy to determine strength, stiffness and toughness properties for structural analysis, 2021. https://repository.tudelft.nl/islandora/object/uuid%3A3bcbbc72-0212-44e9-ac86-2fdc54ec5987.
[23] P. Matysek, T. Stryszewska, S. Kańka, Experimental research of masonry compressive strength in the Auschwitz II - Birkenau former death camp buildings, Eng. Fail. Anal. 68 (2016) 263–274, https://doi.org/10.1016/j.engfailanal.2016.06.007.
[24] C. Demir, A. Ilki, Characterization of the materials used in the multi-leaf masonry walls of monumental structures in Istanbul, Turkey, Constr. Build. Mater. 64 (2014) 398–413, https://doi.org/10.1016/j.conbuildmat.2014.04.099.
[25] E. Franzoni, C. Gentilini, G. Graziani, S. Bandini, Compressive behaviour of brick masonry triplets in wet and dry conditions, Constr. Build. Mater. 82 (2015) 45–52, https://doi.org/10.1016/j.conbuildmat.2015.02.052.
[26] N. Sathiparan, U. Rumeshkumar, Effect of moisture condition on mechanical behavior of low strength brick masonry, J. Build. Eng. 17 (2018) 23–31, https://doi.org/10.1016/j.jobe.2018.01.015.
[27] A.C. Isfeld, M.G. Stewart, M.J. Masia, Structural reliability and partial safety factor assessment of unreinforced masonry in vertical bending, Aust. J. Struct. Eng. 00 (2023) 1–15, https://doi.org/10.1080/13287982.2023.2173868.
[28] NEN-EN 772-16, Methods of test for masonry units - Part 16: Determination of dimensions, (2011).
[29] Municipality of Amsterdam, Archive Technical Drawing of Public Works No 5180, (n.d.). https://archief.amsterdam/inventarissen/scans/5180/2.3.1.5/start/60/limit/10/highlight/9.
[30] NEN-EN 772-1, Methods of test for masonry units - Part 1: Determination of compressive strength, 1 (2022).
[31] DIN18555-9, Testing of mortars containing mineral binders - Part 9: Hardened mortars, determination of the mortar compressive strength in the bed joint, (1999) 1–10.
[32] ASTM C1314–09, Standard test method for compressive strength of masonry prisms, ASTM Int. (2015) 1–10, https://doi.org/10.1520/C1314-09.
[33] J.A. Thamboo, M. Dhanasekar, Correlation between the performance of solid masonry prisms and wallettes under compression, J. Build. Eng. 22 (2019) 429–438, https://doi.org/10.1016/j.jobe.2019.01.007.
[34] NEN-EN1015-11, Methods of test for mortar for masonry - Part 11: Determination of flexural and compressive strength of hardened mortar, 11 (2023).
[35] ASTM E111-17, Standard Test Method for Young's Modulus, Tangent Modulus, and Chord Modulus, (2017) 7.
[36] NEN-EN1052-3, Methods of test for masonry - Part 3: Determination of initial shear strength, 3 (2023).
[37] M.B. Gaggero, R. Esposito, Experimental characterisation of flexural bond behaviour in brick masonry, Mater. Struct. Constr. 56 (2023) 1–17, https://doi.org/10.1617/s11527-023-02144-6.
[38] NEN-EN 1052-5, Methods of test for masonry - Part 5: Determination of bond strength by the bond wrench method, 5 (2022).
[39] N.N. Thaickavil, J. Thomas, Behaviour and strength assessment of masonry prisms, Case Stud, Constr. Mater. 8 (2018) 23–38, https://doi.org/10.1016/j.cscm.2017.12.007.
[40] A. Abasi, R. Hassanli, T. Vincent, A. Manalo, Influence of prism geometry on the compressive strength of concrete masonry, Constr. Build. Mater. 264 (2020), 120182, https://doi.org/10.1016/j.conbuildmat.2020.120182.
[41] J. Segura, E. Bernat, V. Mendizábal, L. Pelà, P. Roca, L. Gil, Experimental comparison of two testing setups for characterizing the shear mechanical properties of masonry, J. Build. Eng. 44 (2021), https://doi.org/10.1016/j.jobe.2021.103277.
[42] J.G. Rots, Structural Masonry: An Experimental/Numerical Basis For Practical Design Rules, CRC Press, 1997.
[43] R. van der Pluijm, Out-of-Plane Bending of Masonry Behaviour and Strength, 1999. doi: 10.6100/IR528212.
[44] T.G. Nijland, J.A. Larbi, R.P.J. van Hees, B. Lubelli, M. de Rooij, Self healing phenomena in concretes and masonry mortars: a microscopic study, in: Proc. First Int. Conf. Self Heal. Mater. 18–20 April 2007, Noordwijk Aan Zee Netherlands, 2007, pp. 1–9.
[45] H. El-Hassan, Y. Shao, Early carbonation curing of concrete masonry units with Portland limestone cement, Cem. Concr. Compos. 62 (2015) 168–177, https://doi.org/10.1016/j.cemconcomp.2015.07.004.